

CARACTERISTICILE TERMICE ȘI PETROFIZICE ALE CALCARENITELOR UTILIZATE ÎN CONSTRUCȚIA DE MOINUMENTE ISTORICE DIN RABAT

THERMAL AND PETROPHYSICAL CHARACTERISTICS OF CALCARENITE ROCKS USED IN THE CONSTRUCTION OF HISTORICAL MONUMENTS OF RABAT

Y. EL RHAFFARI^{1*}, M.HRAITA¹, A. SAMAOUALI¹, M. BOUKALOUCH¹, Y. GERAUD²

¹Laboratory of Thermodynamics, Department of Physics, Faculty of Science, Mohammed V-Agdal University, P.O. Box 1014, Rabat, Morocco.

²Université de Lorraine, Ecole Nationale Supérieure de Géologie, UMR 7359-Géo Ressources
rue du Doyen Marcel Roubault TSA 70605, 54518 Vandoeuvre Les Nancy Cedex, France

This paper presents a study on the thermal and petrophysical characteristics of porous calcarenites, sampled from a quarry located near the historical monument of Chellah (Rabat).

We measured the thermal conductivity using box method and Thermal Conductivity Scanner (TCS). The sample's thermal conductivity map generated by exploiting the values produced by (TCS), gives a clear view of the thermal heterogeneity of the studied rock.

The measurement of mercury intrusion porosimetry shows two porous networks (macropores and micropores); the value of porosity is between 16,52% and 34,9%. We have also found that porosity is one of the main parameters that control the transfer of heat in the calcarenites of Rabat.

Keywords: calcarenites, thermal conductivity, mercury intrusion porosimetry, box method, TCS method

1. Introduction

The first traces of the use of the Moroccan construction stones go back to Roman times and are located near the ancient cities of Volubilis, Lixus, Chellah. Ancient massive extractions date back to the time of the Almohads (XII-XIII century) and are particularly the calcarenites as well as the consolidated and metamorphosed limestones, which were used in the construction of their main historical monuments [1].

Degradation of monumental stones is an unavoidable phenomenon that has been accelerated under the effect of humidity and urban pollution. Rocks are disintegrated by various physical, chemical, mineralogical, petrophysical and mechanical processes.

The thermal conductivity of a geo-material (stone, rock) depends on its porosity and its mineralogy, these two characteristic parameters of the material evolve with alteration [2,3]. The measurement of the thermal conductivity can be used to characterize the alteration of the material. Indeed, the thermal fluctuations (daily and seasonal) decrease its quality and can also be the cause of fractures of the material's microstructure. Some minerals have a high anisotropy of the

thermal expansion, particularly the calcite which has a high expansion in its main axis but a contraction in its direction perpendicular [4].

In this paper we study the thermal and petrophysical behavior of a calcarenite rock from Rabat (Morocco). The study focuses on the measurement of the thermal conductivity by the box method and the thermal conductivity scanner TCS as well as a petrophysical analysis using mercury intrusion porosimetry.

Heat transfer in a heterogeneous material is influenced by various factors, such as the distribution of solid phases, pores, and cracks. There are many models which express the thermal conductivity taking into account the geometry and distribution of the pores. In this study, we have adopted a porosity model as a function of the thermal conductivity average values of the sample heterogeneity.

The results identify the nature of the calcarenite stone used in the construction of historical monuments of Rabat city. They show that the studied rock presents an important thermal and petrophysical heterogeneity. We have also demonstrated that the thermal conductivity depends on porosity.

* Autor corespondent/Corresponding author,
e-mail: ayounes1@hotmail.com

2. Description of method of work

2.1. Sampling

The materials used in archeological Chellah site are numerous; one finds various limestones, granite, red bricks of various periods as well as cob. In this study, we were interested in materials used mainly in the Roman part for the current buildings and in the Islamic part for the monumental doors.

These materials correspond to calcarenite stone, which is the stone most commonly used in the construction of the historical monuments in the city of Rabat. They are located between Casablanca and Larache (Morocco) (Figure 1). [2,5-7].

Geologically, it is a calcareous limestones, of Plio-Quaternary age in the form of a system of dune ridges running parallel along the Atlantic coast. The deposit calcarenite took place under the action of a substantially aeolian dynamics with plenty of round quartz grains mats which remobilized sand beach, and by the large horizontal stratifications [8]. Chemical analyzes of several samples of calcarenites Plio-Quaternary in the city of Rabat indicate that the main component of these deposits is calcium carbonate (CaCO_3), its content varies between 50 and 57%, reflecting the importance of bioclasts marines. In contrast, the content of silica (SiO_2), which is in the form of quartz grains, is very low [6,9,10].

The E tested sample is a calcarenite stone block of $(27 \times 27 \times 4) \text{ cm}^3$ dimensions (Figure 2), sampled from a quarry located near the historical monument of Chellah (Figure 3). Indeed, the most monuments are protected by the Moroccan authorities in order to keep their value and importance.

2.2 The box method

The measuring cell EI-700, named the box method, is particularly designed to determine the thermal conductivity and diffusivity. This method, developed in the Laboratory of Solar and Thermal Studies of Claude Bernard University Lyon 1 [11-14], includes:

- A strongly isolated chamber "A" is maintained at a low temperature (-4°C) by cooling water, coming from a cryostat.

- Two identical measuring boxes, which are independent and isolated from the inside by polystyrene, allow the measurement on the samples of $(27 \times 27 \times 4) \text{ cm}^3$ dimensions.

One box is for the measurement of thermal conductivity in a steady state, the other one is for the determination of thermal diffusivity in a transient state.

The measurement of the thermal conductivity by the box method, in a steady state, consists of making two atmospheres one of them is hot and the other is cold from both sides of the



Fig. 1 - Map of Morocco.



Fig. 2 - Digital image of E Sample $(27 \times 27 \times 4) \text{ cm}^3$.



Fig 3 - The quarry is to the altitude of 56 m (latitude: 33,944499, longitude: -6, 729126)
 (a) Zone of quarry where the calcarenite rock (b) has been taken.
 (b) The rock from which the samples (dimensions: $270 \times 270 \times 40 \text{ mm}^3$) were cored.

tested sample: A chamber “A” is strongly isolated at a low temperature; and a box B is equipped with a heating film which is controlled by a rheostat that maintains temperature T_b near the ambient temperature T_a (Figure 4).

The surface temperatures of the sample, the temperatures of the hot and cold atmospheres, and the ambient temperature are all measured by a Type K thermocouple.

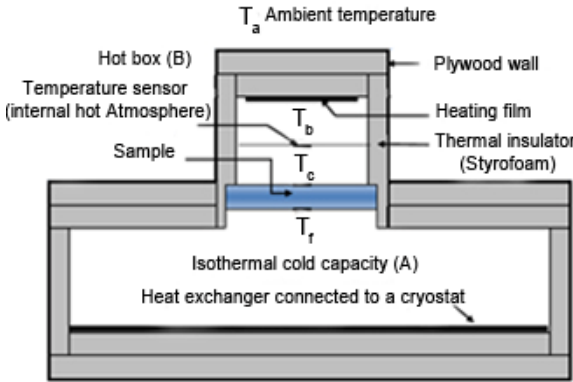


Fig. 4 - Thermal conductivity measuring Box

The value of the thermal conductivity λ_a ($W \cdot m^{-1} \cdot K^{-1}$) is calculated using the following expression:

$$\lambda_a = \frac{e}{S_T (T_c - T_f)} \left[\frac{V^2}{R} - C(T_b - T_a) \right] \quad (1)$$

- S_T : Sample Surface (m^2)
 - T_c : Temperature of the hot surface ($^{\circ}C$)
 - T_f : Temperature of the cold surface ($^{\circ}C$)
 - T_a : Ambient temperature ($^{\circ}C$)
 - T_b : Temperature of the hot atmosphere ($^{\circ}C$)
 - e : Sample Thickness (m)
 - V : Voltage across the heating resistance element (V).
 - R : Heating resistance element (Ω)
 - C : Coefficient of heat loss ($W \cdot C^{-1}$)
- The overall loss coefficient C is given by the manufacturer of the device: $C = 0.16 W \cdot C^{-1}$.

2.3 TCS Method (Thermal Conductivity Scanner)

The technique presented below is based on the temperature variation of the sample surface resulted from a known and controlled heat report. The device is therefore in the form of a mobile

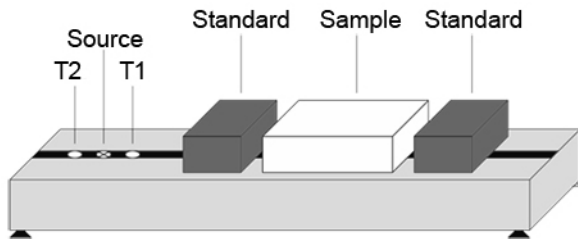


Fig. 5 - Thermal Conductivity Scanner (TCS).

element composed of two temperature sensors and a heat source, aligned parallel to the axis of movement, so that we can measure the temperature of the sample before and after heating. This block moves at a constant speed near the sample surface, along a measuring line and thus allows obtaining a profile of thermal conductivity (Figure 5).

The sample preparation is relatively simple. To avoid a variation of absorption of heat due to the variations of colors on the surface of the sample, a black coat of paint is applied to the sample so that its coefficient of absorption is close to the unity. The range of the measurable conductivities is between $0,2$ and $70 W \cdot m^{-1} \cdot K^{-1}$, the error of measure is less than or equal to 2 % [15 -17].

To get a map of thermal conductivity, the sample is carefully positioned in the apparatus; the scanner gives the thermal conductivity measurement for each profile (a sample line) by scanning millimeter by millimeter.

2.4 Mercury intrusion porosimetry

Different techniques are used to estimate the values of porosity and highlight geometric properties of the porous network [18,19]. In this work, the technique used is the Mercury intrusion porosimetry.

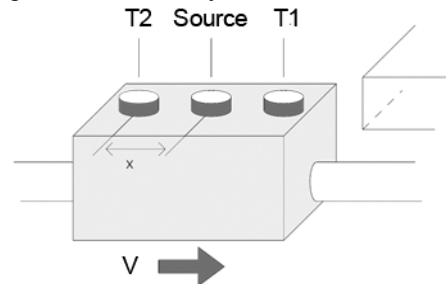
Mercury is a non-wetting fluid, the contact angle between mercury and the surface of the sample is greater than 90° . It is therefore necessary to apply a pressure on mercury to penetrate it inside the porous network. According to the law of Laplace and Young, the relationship between the capillary radius and the pressure applied is:

$$P_c = \frac{2\sigma \cos \theta}{R_c} \quad (2)$$

With:

- θ : Contact angle between mercury and solid, $\theta = 140^{\circ}$ for non-wetting fluid
- σ : Air-mercury interfacial tension ($0,486 N/m$ at $25^{\circ}C$)
- R_c : The radius of the capillary tube (μm) [2,20]
- P_c : Mercury pressure (bar)

The capillary pressure is the pressure difference between the non-wetting fluid and the wetting fluid for mercury is:



$$P_c = P_{Hg} - P_{vap} \quad (3)$$

The mercury vapor pressure cannot exceed the saturation vapor pressure of mercury which is 0,002 Torr ($\approx 2,6$ Pa) at ambient temperature (25 °C), we can approximate the capillary pressure using the mercury pressure injected fluid :

$$P_c \approx P_{Hg} \quad (4)$$

Thus, each pressure corresponds to a pore radius of access. Replacing the constant σ and θ by their values in the equation (2), we obtain the following relationship:

$$P_{Hg} = \frac{7,5}{R_c} \quad (5)$$

P_{Hg} in bar and R_c in μm .

These porosimetry measurements are performed using an apparatus Micromeritics Pore Sizer 9320 which makes it possible to inject mercury with pressures ranging between 0.001 and 300 MPa. So, the access threshold ranges between 400 and 0.003 μm . This technique determines the connected porous volume and its distribution according to the injection pressure and the thresholds access.

Cylindrical samples, of 10 mm length and 17 mm in diameter, were dried at 60°C, weighed and placed in an injection cell. After a degasification step under a 50 μm mercury depression, the injection cell is filled with mercury, and then the vacuum is broken gradually until atmospheric pressure. The intrusion measurement, i.e. the volume of mercury injected into the sample, is made for low pressures (between 0.001 and 0.15 Mpa) and for high pressures (between 0.15 and 300 Mpa). The pressure rises are carried out in stages; after each stage, the injected mercury volume is measured. From these data, it is possible to determine the saturation curve according to the injection pressure. The precision of the measurements is about 4%.

3. Results, interpretations and discussion

3.1 Thermal conductivity:

The measurement of the thermal conductivity by the box method is made in a steady state and requires a relatively large time (≈ 4 hours). The measurement error, given by the manufacturer of the apparatus, is 10%.

The value of the apparent thermal conductivity of the sample E, measured by box method, is:

$$\lambda_a = 1,7 \pm 0,1 W.m^{-1}.K^{-1} \quad (6)$$

3.2 Thermal conductivity map:

270 Thermal profiles were performed on sample E; the data is stored in an MS Excel workbook as a square matrix of 255 x 255 cells. The values of a matrix line represent the profile of the thermal conductivity along a line of the sample.

15 lines have been omitted to avoid side effects. We calculated the average value of the thermal conductivity λ_m of the sample based on all the values of the matrix:

$$\lambda_m = 1,73 \pm 0,02 W.m^{-1}.K^{-1} \quad (7)$$

We find that the value of the apparent thermal conductivity measured by box method (6) is consistent with the value of the effective thermal conductivity determined by TCS (7).

The sample's thermal conductivity map has been generated by exploiting the values of the matrix, using a Matlab program (Figure 6).

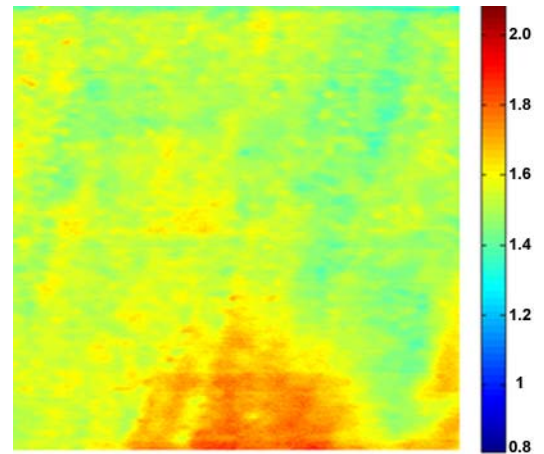


Fig. 6 - Map of sample E thermal conductivity.

The Thermal map, produced by TCS, shows the distribution of the values of the thermal conductivity on the sample surface. The enclosed color scale shows a fairly large dispersion of the thermal conductivity values and thus gives a clear view of the thermal heterogeneity of the studied rock. Therefore, the mass distribution is not uniform on the surface of the sample; high conductivity region has high surface density.

3.3 Mercury intrusion porosimetry

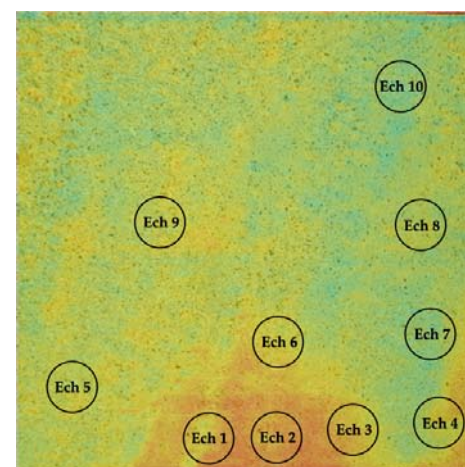


Fig. 7 - The areas of 10 cylindrical samples to be studied.

To confirm the profiles obtained on the thermal map and to better understand the porous structure, we have superimposed the digital image of the sample E on the thermal map, using an image processing tool which allows us to select the areas to be studied (Figure 7). To perform the analysis by the mercury intrusion porosimetry method, 10 cylindrical samples were extracted by an electric core drill with a diamond crown cooled by water (Figure 8).

The results of the mercury porosity analysis of each cylindrical sample are represented on two types of graphs:

- The curves in a logarithmic scale represent the cumulative injected mercury volume as a function of the distribution of pore access ray.
- The curves represent the injected mercury volume for each pore access ray.

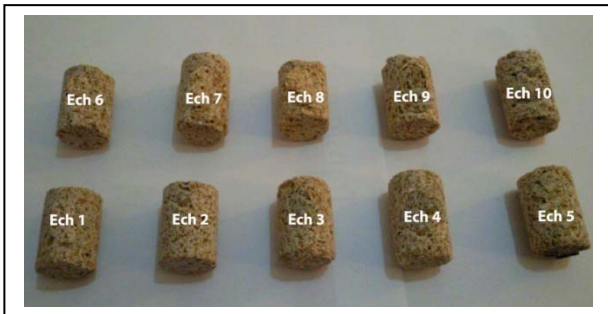


Fig. 8 - Ten cylindrical samples extracted by coring.

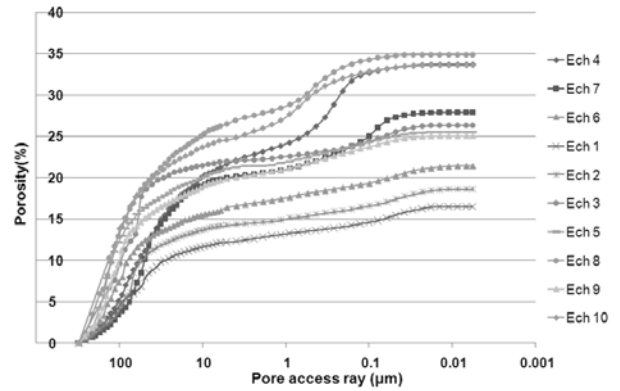


Fig. 9 - The mercury injection Curves for 10 samples.

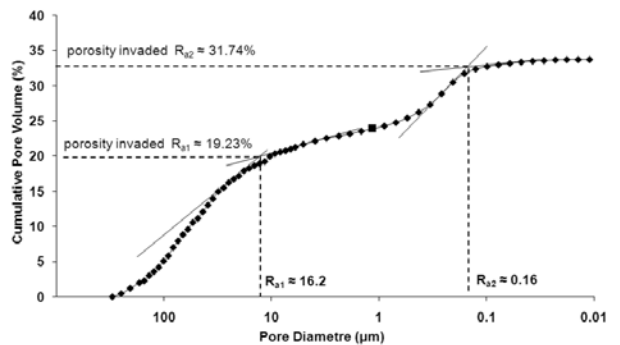


Fig. 10 - Tangent method to determine graphically the thresholds access of the pores.

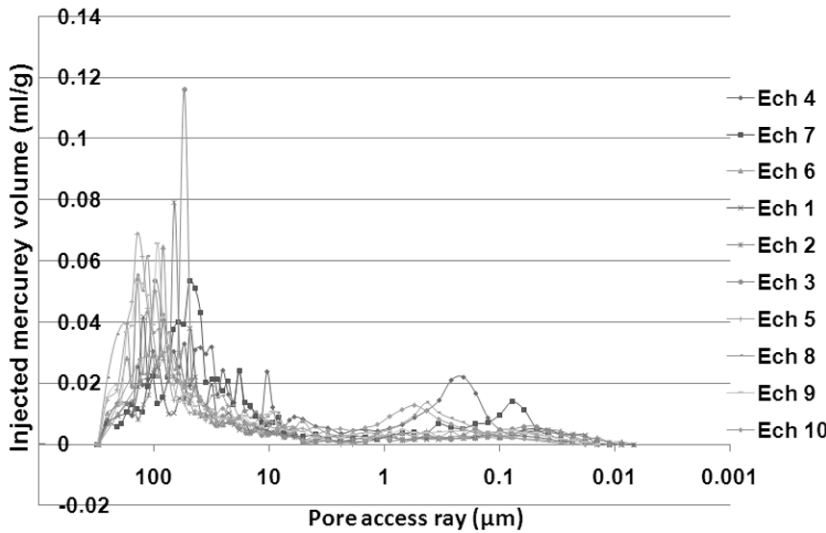


Fig. 11 - The injected mercury volume for 10 samples.

The mercury injections Curves contain two inflection points (Figure 9). It explains that the pore volumes distribution of the sample E is bimodal (two families of pores are dominant). Graphically by the tangent method (Figure 10), we can determine two thresholds pores R_{a1} and R_{a2} corresponding to the access pores rays which for a weak increment pressure give access to a large pore volume [21 - 24]. These results are confirmed by the calculated dispersion coefficient C_d equals 1,2 for all samples [18,19,25,26].

$$C_d = \frac{P_{80} - P_{20}}{P_{50}} = \frac{R_{20} - R_{80}}{R_{50}} \quad (8)$$

P_{20} , P_{50} and P_{80} are injection pressures and R_{20} , R_{50} and R_{80} are access radius correspond to the invasion of 20%, 50% and 80% of the porous media respectively.

On the curves representing the injected mercury volume for each pore access ray, two thresholds pores are observed (Figure 11).

Table 1

The results of the analysis by the mercury intrusion porosimetry

Samples	Porosity (%)	Thresholds of the pores $R_{a1}(\mu\text{m})$	Thresholds of the pores $R_{a2}(\mu\text{m})$
Ech 1	16.52	16.2	0.027
Ech 2	18.62	28.03	0.022
Ech 3	26.37	25.14	0.037
Ech 4	33.74	16.2	0.16
Ech 5	25.52	74.26	0.037
Ech 6	21.45	60.91	0.022
Ech 7	27.94	15.64	0.06
Ech 8	34.9	39.22	0.126
Ech 9	25.07	54.41	0.037
Ech 10	33.58	46.85	0.262

Table 2

Values of the average thermal conductivity of each area of the E sample surface as function of the values of the porosity

Samples	Ech 1	Ech 2	Ech 3	Ech 4	Ech 5	Ech 6	Ech 7	Ech 8	Ech 9	Ech 10
λ ($\text{W}\cdot\text{m}^{-1}\cdot\text{K}^{-1}$)	1.78	1.87	1.66	1.52	1.53	1.62	1.35	1.45	1.53	1.32
Porosity (%)	16.52	18.62	26.37	33.74	25.52	21.45	27.94	34.9	25.07	33.58

These curves show two populations of pores, forming two porous networks: macropores and micropores.

We observe a strong increase in porosity for macropores (from 5 to 300 μm) and a medium increase for micropores (0.01 to 1 μm). So, it can be concluded that the most dominant population is the macropores.

In macropores family, the values of the thresholds access of the pores are between 15.64 μm (Ech 7) and 74.26 μm (Ech 5). In micropores family, the minimum value is 0.022 μm (Ech 2 and Ech 6), while the maximum value is 0.262 μm (Ech 10) (Table 1).

Porosity of the studied rock is between 16,52% (Ech 10) and 34,9% (Ech 8).

3.4 Porosity in relation to thermal conductivity

For each cylindrical sample, we have calculated the average of the thermal conductivity from the Excel matrix determined by TCS (Table 2). Figure 12 shows the values of the porosity as function of the average thermal conductivity of the ten samples. The results obtained show that the porosity decreases when the thermal conductivity increases.

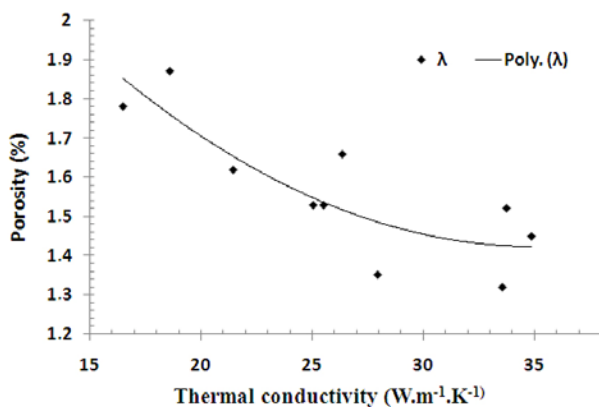


Fig. 12 - Porosity of the E sample surface as function of the average thermal conductivity.

4. Conclusion

In this paper, we have examined the thermal and petrophysical behavior of a calcarenite sample E. This type of rock is often used as construction material of Rabat historical monuments (Morocco).

The value of the apparent thermal conductivity determined by box method is in accordance with the average value of thermal conductivity obtained by the optical method TCS.

The thermal conductivity profile obtained by TCS method shows clearly the mass heterogeneity of sample E. The low thermal conductivity areas correspond to the areas of high porosity and vice versa.

The results obtained by mercury porosity method have revealed more information about the petrographic structure of the sample E. They have shown a bimodal pore network where two pore access ray families coexist (micropores and macropores). We have concluded then that macropores are more dominant than the micropores.

Porosity is one of the main parameters that affect the transfer of heat and mass in the calcarenites of Rabat. The heat transfer is very sensitive to the structural heterogeneities as well as the chemical composition of the material.

Acknowledgments

This work was supported by the French-Moroccan cooperation within the project named (PAI Volubilis) N° MA/07/168.

REFERENCES

1. I. El Amrani El Hassani, and H. El Azhari, Evaluation des propriétés physico-mécaniques des pierres de construction du Maroc à partir des vitesses des ondes P et de la résistance au choc, Bulletin de l'Institut Scientifique, section Sciences de la Terre, Rabat, 2009, **31**, 41.
2. A. Samaouali, L. Laânab, M. Boukalouch, and Y. Géraud, Porosity and mineralogy evolution during the decay process involved in the Chellah monument stones, Environ Earth Sci, 2010, 59:1171–1181, DOI 10.1007/s12665-009-0106-5.

3. R. Ezzdine, Phd thesis, Endommagement des monuments historiques en maçonnerie, Université bordeaux 1-école doctorale des sciences physiques et de l'ingénieur, N° d'ordre : 3787, France, 2009.
4. A. Kieslinger, Les principaux facteurs d'altération des pierres à bâtir, ICOMOS, Pologne, 1968, **2** (3), 63.
5. M. Akil, Phd thesis, Les dépôts quaternaires littoraux entre Casablanca et cap Beddouza: Etudes Géomorphologiques et Sedimentologiques, University Mohamed V of Rabat, Morocco, 1990.
6. H. Azouaoui, N. El Hatimi, and N. El Yamine, Plio-Quaternary formations of the Casablanca area (Morocco): sedimentological and geotechnical aspects, Bull Eng Geol Environ, 2000, **59**, 59.
7. N. Zaouia, M. ELwartiti and B. Baghdad, Superficial alteration and soluble salts in the calcarenite weathering. Case study of almohade monument in Rabat: Morocco, Environ. Geol, 2005, **48**, 742.
8. M. Maanan, Phd thesis, Etude sédimentologique du remplissage de la lagune de sidi moussa (côte atlantique marocaine) caractérisations granulométrique, minéralogique et géochimique, Université chouaib doukkali of el jadida, Morocco, 2003.
9. R. Benboughaba, Phd thesis, Etude Sédimentologique et Géophysique des formations littorales plio-quaternaires de l'axe Rabat-Kénitra(Maroc), Université Mohammed V of Rabat, Morocco, 2001.
10. A. Samaouali, L. Laâna, Y. Geraud, A. Nounah, and M. Boukalouch, Experimental study of chemical deterioration of chellah monument stones, Phys. Chem. News , 2008, **44**, 103.
11. M. Rhzioual Berrada, Phd thesis, Identification des caractéristiques thermophysiques des principaux matériaux locaux de construction au Maroc : Application à la valorisation du stérile de phosphate, University Mohammed V of Rabat, Morocco, 2000.
12. Y. El rhaffari, M. Boukalouch, and A. Khabbazi, Conductivité et diffusivité thermiques des matériaux poreux : Application aux pierres du monument historique Chellah, in Proceeding of the congress Matériaux 2010, Nantes, Octobre 2010, (840), 360.
13. M. Z. Bessenouci, Approches théoriques de la conductivité thermique apparente du béton de pouzzolane à l'aide d'une modélisation des matériaux poreux, Revue des Energies Renouvelables, 2011, **14** (3), 427.
14. A. El Bouardi, H. Ezbakhe, T. Ajzoul and V. Wittwer, Propriétés thermophysiques lors de changement de structure granulaire - compact. Mesures et identifications; application aux matériaux à matrice déformable et expansé à l'air : cas de la vermiculite et polystyrène, 12^{èmes} Journées Internationales de Thermique, Tanger, 2005, 311.
15. Y.A. Popov, D. Pribnow, J.H. Sass, C.F. Williams and H. Burkhart, Characterisation of rock thermal conductivity by High resolution Optical scanning, Geothermic, 1999, **28**, 253.
16. M. Rosener, Transfert de chaleur entre fluides et roches, exemple du site géothermique de Soultz-Sous-Forêts, Phd thesis, University Louis Pasteur of Strasbourg, France, 2007.
17. A. Samaouali, Processus d'altération et de transfert de fluides dans les pierres calcarénites du monument Chellah-Rabat, Phd thesis, University Mohammed V of Rabat, Morocco, 2011.
18. Y. Geraud, Phd thesis, Déformation thermomécanique et porosité des roches granitiques. Evolution des espaces poreux, Université de Provence (Aix-Marseille I) of Marseille, France, 1991.
19. C. Thomachot, Phd thesis, Modifications des propriétés pétrophysiques de grès soumis au gel ou recouverts d'encroûtements noirs vernissés, University Louis Pasteur of Strasbourg, France, 2002.
20. E.W. Washburn, The dynamic of capillary flow, Phys. Rev., 1921, **17** (3), 273.
21. A.J. Katz and A.H. Thompson, Quantitative prediction of permeability in porous rock, Physical Review, 1986, **34.7**, 8179.
22. J.D. Mertz, Structures de porosité et propriétés de transport dans les grès, Sciences Géologiques, 1991, (90), University Louis Pasteur of Strasbourg, France.
23. E. D. Pittman, Relationship of porosity and permeability to various parameters derived from mercury injection-capillary pressure curves for sandstone, Amer. Assoc. Petrol. Geol. Bull., 1992, **76** (2), 191.
24. T. B. Rousset, Transferts par capillarité et évaporation dans des roches : rôles des structures poreuses, Université Louis Pasteur of Strasbourg, France, 2001.
25. J.M. Remy, Phd thesis, Influence de la structure du milieu poreux carbonaté sur les transferts d'eau et les changements de phase eau-glace. Application à la durabilité au gel de roches calcaires de Lorraine, Institut National Polytechnic of Lorraine, France, 1993.
26. N.C. Wardlaw, M. Mckellar, and Y. Li, "Pore and throat size distributions determined by mercury intrusion porosimetry and by direct observation", Carbonates and Evaporites, 1988, **3** (1), 1.
